Mechanism of sequential switching of current filaments in an avalanche S-diode

© I.A. Prudaev[1], V.V. Kopyev[1], V.L. Oleinik[1], V.E. Zemlyakov[2]

[1] Tomsk State University,
63405 Tomsk, Russia
[2] National Research University of Electronic Technology,
124498 Zelenograd, Moscow, Russia

E-mail: funcelab@gmail.com

Received May 21, 2024
Revised August 13, 2024
Accepted August 14, 2024

The paper presents the results of a study of a sequential switching of current filaments in an avalanche S-diode with deep iron centers. It has been experimentally shown that at a high repetition rate (100 kHz), the current filaments are distributed over the area of the electron-hole junction more uniformly compared to switching at a low frequency (100 Hz). In this case, the switching voltage at the first switching event of the avalanche S-diode is always higher than at the second one. To analyze the results, a numerical experiment on the formation of a locally heated region with an increased concentration of nonequilibrium carriers was proposed. Simulation of the dynamics of carrier redistribution under conditions of nonuniform heating of the S-diode allows one to propose a new mechanism for sequential switching of current filaments. In this mechanism, the recharging of deep centers in the vicinity of each previous current filament sets the conditions for the formation of each subsequent switching channel.

Keywords: thermal conductivity, gallium arsenide, deep centers, current filament.

DOI: 10.61011/SC.2024.07.59546.6718

1. Introduction

Avalanche S-diode — is a closing switch operating by generating the ionizing collapsing domains (CD) in GaAs [1–4]. CD mechanism was discovered during numerical modelling of switching the avalanche bipolar transistors (ABT) from GaAs [5–7] and further was used to explain the super-fast switching of the photovoltaic switches HG PCSS (High Gain Photoconductive semiconductor switch) from GaAs [8–10], avalanche S-diodes [4] and sharpening diodes from GaAs [11–13]. The drastic decrease of the switch resistance in CD mode (switching time about $0.1-1$ ns) occurs due to an avalanche generation of the charge carriers by multiple ionizing domains, mooving from the cathode to the anode [5].

In practical terms, the operation of switches in the current pulse repetition mode is of some interest. Thus, for 3D-lidars when pumping the semiconductor lasers a frequency of dozens-hundreds of kHz is used, which may be implemented by using the avalanche S-diode [4]. However, the numerical analysis of frequency dependencies for the avalanche S-diodes is somewhat complicated because of the circumstances described below. Switching there always occurs in the current filament, the location of occurrence of which seems, at first glance, quite unpredictable and relating to the non-controlled heterogeneity (impurity fluctuation, second phase inclusions in the bulk area or in GaAs [14]). There are no papers in the literature where it is explained why the current filaments originate in the mode of sequential triggering of the electronic avalanche switch containing deep centers (in particular, avalanche S-diode doped with a deep acceptor — iron).

In this paper the experimental results are provided to visualize the current filaments in the avalanche S-diodes, indicating the interrelation between the two sequential switching at high pulse-repetition rates (frequencies). To explain the results a numerical experiment was suggested and carried out with 2D simulation of a local heating and generation of the non-equilibrium charge carriers in S-diode. In this paper, it is shown that at high repetition frequencies, when the semiconductor structure does not have enough time to transit to an equilibrium state, an area with the most favorable conditions for subsequent avalanche breakdown is formed near the current filament. The formation of this region occurs under heterogeneous recharge of the deep impurity in the vicinity of the current filament and local heating of GaAs lattice.

2. Experiment procedure

The studied S-diodes were fabricated from GaAs-structure of $n^+-\pi-n-n^+$-type. It should be clarified, that this structure, in fact, is a transistor structure, but it has only 2 electrodes [4]. The areas of π- and n-type contained a deep iron acceptor impurity with a concentration of $(2-10)\cdot 10^{16}\,\mathrm{cm}^{-3}$. The structure and triggering circuit of S-diode are described in details in paper [3]. In the experiment for the visualization of current filaments the standard equipment described in paper [5,13] was used, the

observation was carried out from the top contact of S-diode ($n^+-\pi$-junction). Illumination of conductivity channels (during radiative recombination) was registered in the infra-red band using camera WATEC WAT-933. Due to high camera sensitivity a glowing from a single current filament may be observed. Major difference of the applied technique from the technique described in papers [4,5,13], was channels observations in the mode of generation of a pulse burst (number of pulses in the burst varied from 1 to 100, frequency of pulses in the burst — from 1 to 100 000 Hz). Parallel with observation of channels glowing the switching voltage of the avalanche S-diodes was measured, for which the 500 MHz oscilloscope was used.

3. Experimental findings

Figure 1 shows the results of visualization of current filaments. Figure 1, *a* schematically shows the geometry of studied S-diodes. Observation of glowing of single current pulses showed that for various samples there may be different number of channels: from 0 to 2. This indicates the possible inclusion of current filaments under the contact (when they are not observed in the experiment) and possible synchronization of several channels with a single connection (when 2 optical spots are observed). Similar conclusions were made during the study of the sharpening diodes GaAs [13].

The rise in the number of pulses at low frequency didn't result in higher spots amount. Thus, at 100-fold switching at a frequency of 100 Hz the number of glowing spots was no higher than two (Figure 2). Their brightness is significantly higher compared to the picture with single switching, which is explained by the integration of the signal in the camera used. Thus, at low frequency, when enough time passes between two adjacent switchings in time to establish an equilibrium state, the channels always originate in the same places. It is natural to assume that these places are due to the presence of fluctuations in the composition (shallow or deep donor impurity, inclusions of the second phase [14]).

Principally different behavior of structure is observed at high frequency. At 5-fold switching at 100 kHz the glowing pattern looks a bit more distributed compared to the single switching. And in case of 100-fold switching at a frequency of 100 kHz practically uniform glowing is observed allowing to see the entire mesa of S-diode in the infra-red band. At that, it should be noted that from one burst of pulses to another the intensity distribution for one and the same S-diode varies. This indicates the presence of an individual path of sequential activation of channels (the process of generation of current filaments is not rigidly deterministic).

Since the avalanche breakdown voltage rises with the growth of temperature, the result could be explained by heating within each current filament. At high frequencies when the heated area cannot quickly cool down, the avalanche breakdown voltage becomes higher to the moment of next switching of S-diode. And this shall lead to

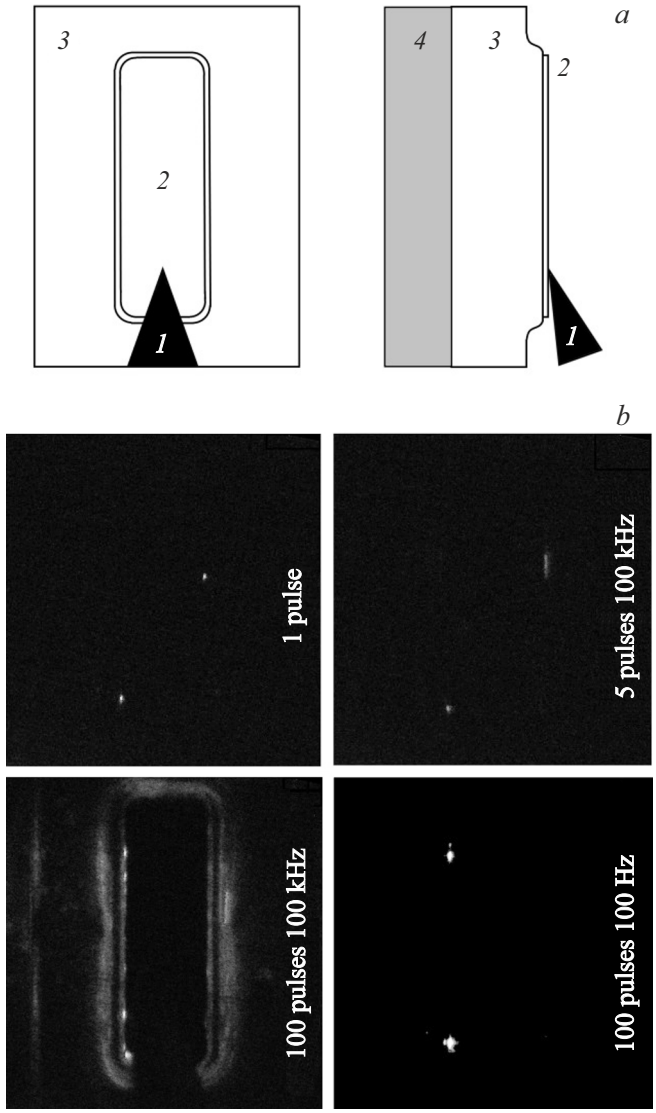

Figure 1. Schematic diagram of S-diode from the top and side (*a*) and photos of S-diode from the top in the infra-red band at various switching conditions (*b*). *1* — press contact, *2* — upper metallic contact of S-diode with a size of $0.3 \times 1\,\text{mm}^2$ (on $n^+-\pi$-junction side), *3* — GaAs crystal, *4* — lower metallic contact.

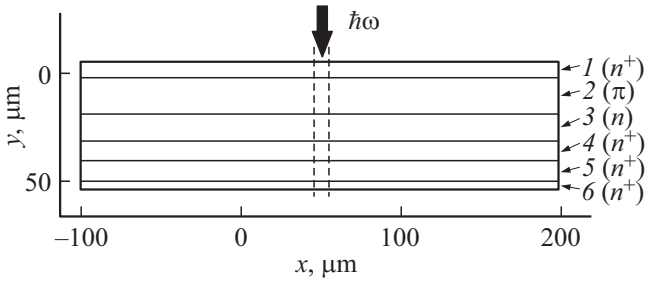

Figure 2. Schematic image of 2D-model of avalanche S-diodes. Absorption coefficient in layers *2–4* is much higher than absorption coefficients in layers *1, 5* and *6*. Thermal conductivity coefficient of layer *6* is 100 times lower than thermal conductivity coefficient of layers *1–5*. Dashed lines indicate the boundaries of the light beam.

triggering of the next more cold region of *S*-diode. In this case the voltage of second switching of *S*-diode should increase at least gradually but shall not decrease relative to the first switching. However, an opposite effect was observed in our experiment. The experiments performed in this study demonstrated that in respect to the first pulse the voltage during second switching was always by 8–14% lower at a frequency of 100 kHz. The amplitude of the subsequent pulses varied slightly. To explain the results obtained, a mechanism was proposed allowing for the recharge of a deep acceptor center of iron. Qualitative description of this mechanism is given further.

After the current filament with a concentration of carriers $10^{19}\,\mathrm{cm}^{-3}$ is formed (according to papers for ABT [5–7]) a quick capture of holes on the negatively charged iron centers occurs, which results in neutralizing of the acceptor impurity. The concentration of initially charged centers in π-area is $10^{16}\,\mathrm{cm}^{-3}$. In addition, in parallel with the capture process, charge carriers recombine through centers located close to the middle of the band gap (e. g., through EL2 centers [2]). Thus, the concentration of free electron-hole pairs decreases rapidly by several orders of magnitude. As a result, in place of the current filament, the concentration of nonequilibrium electrons remains higher than the holes concentration for a long time, until the iron centers are completely filled with electrons.. If the subsequent activation occurs before the full capture of electrons, then the avalanche breakdown voltage should decrease, since the rate of avalanche generation depends on the product of the impact ionization coefficient by the concentration of free charge carriers. Localization of region with recharged iron impurity is dependent from many processes: recombination, inhomogeneous heating, diffusion and drift in an embedded field. Accounting for all processes requires solving a system of equations of Poisson, continuity and heat.

4. Description of model and simulation results

For the analysis, the charge carriers distribution and the crystal lattice temperature for the two-dimensional structure of *S*-diode over time was simulated. Since two-dimensional simulation in CD generation mode seems to be an unsolvable task at this stage (due to the lack of huge computational resources), another method for the formation of a local heated region with an electron-hole plasma in a numerical experiment was proposed. In particular, local heating and generation of the non-equilibrium carriers are provided due to absorption of light in GaAs. This method is selected because approval of this mechanism requires simulation only after switching off the current, i. e. without electric field.

TCAD Sentaurus software was used in simulation. This software performs a simulated physical modeling of the process which is initiated at the initial equilibrium state of the system. To create the necessary distribution of charge carrier concentration and temperature, the sample was divided into layers with different absorption coefficients and thermal conductivity coefficients. The structure of the sample is shown in Figure 2. In the numerical experiment the sample was locally irradiated by the optical radiation pulse with a duration of 3 ns and front edges of 500 ps, which is close to the switching time of *S*-diodes in the high-current mode [4]. The optical spot diameter was set as $10\,\mu$m according to experimental data (in experiment the diameter was $10-20\,\mu$m for the avalanche *S*-diodes [4]). The impurity distribution was irrespective of the coordinate x. To solve the optical problem, the structure was divided into subdomains with various absorption coefficients, which made it possible to locally increase the concentration only in the active area of the device. When tackling the thermal problem, the thick layer of the substrate was replaced by a layer with a lower thickness and thermal conductivity relative to the experimental samples (both parameters were reduced by 100 times). The temperature on the substrate bottom side was $T = 300\,\mathrm{K}$, which was consistent with the experiment. Only such conditions were selected where the heating in the filament area ΔT was $\sim 100\,\mathrm{K}$, and concentration of the non-equilibrium carriers — $10^{19}\,\mathrm{cm}^{-3}$ (these data were selected from the ABT simulation studies [5–7]). The transient process dynamics was modelled in the time interval from 10^{-12} to 10^{-3} s.

The thermodynamic model was used in the calculations. In this case, in addition to the Poisson and continuity equations, the following nonstationary heat equation was solved for electrons and holes [15]:

$$c_V \frac{\partial T}{\partial t} - \nabla k \nabla T = -\nabla\left[\left(\alpha_n T - \frac{\mathrm{F}_n}{e}\right)\mathbf{J}_n + \left(\alpha_p T - \frac{\mathrm{F}_p}{e}\right)\mathbf{J}_p\right] - \left(E_C + \frac{3}{2}kT\right)\nabla \mathbf{J}_n/e - \left(E_V - \frac{3}{2}kT\right)\nabla \mathbf{J}_n/e + R(E_C - E_V + 3kT) + (\hbar\omega - E_g)G^{\mathrm{opt}}, \quad (1)$$

where $T = T(x, y)$ — temperature, $c_V = 1.6\,\mathrm{J/(K \cdot cm^3)}$ — volumetric heat capacity, $\kappa = 0.46\,\mathrm{W/(K \cdot cm)}$ — thermal conductivity coefficient (for the substrate layer — $4.6\,\mathrm{mW/(K \cdot cm)}$), α — thermopower factor, F — Fermi energy, J — density of electric current, $E_{V,C}$ — edge energies for permitted bands, R — recombination rate (Shockley–Read mechanisms, radiative and Auger-recombinations are taken into account), e — electron charge, k — Boltzmann constant, $\hbar\omega$ — energy of absorbed photons, G^{opt} — rate of optical regeneration, E_g — width of band gap GaAs, symbols n and p denote the electrons and holes.

The density of electric current is calculated within the model as follows [15]:

$$\mathbf{J}_n = -en\mu_n\left(\alpha_n \nabla T - \nabla \frac{\mathrm{F}_n}{e}\right),$$

$$\mathbf{J}_p = -ep\mu_p\left(\alpha_p \nabla T - \nabla \frac{\mathrm{F}_p}{e}\right). \quad (2)$$

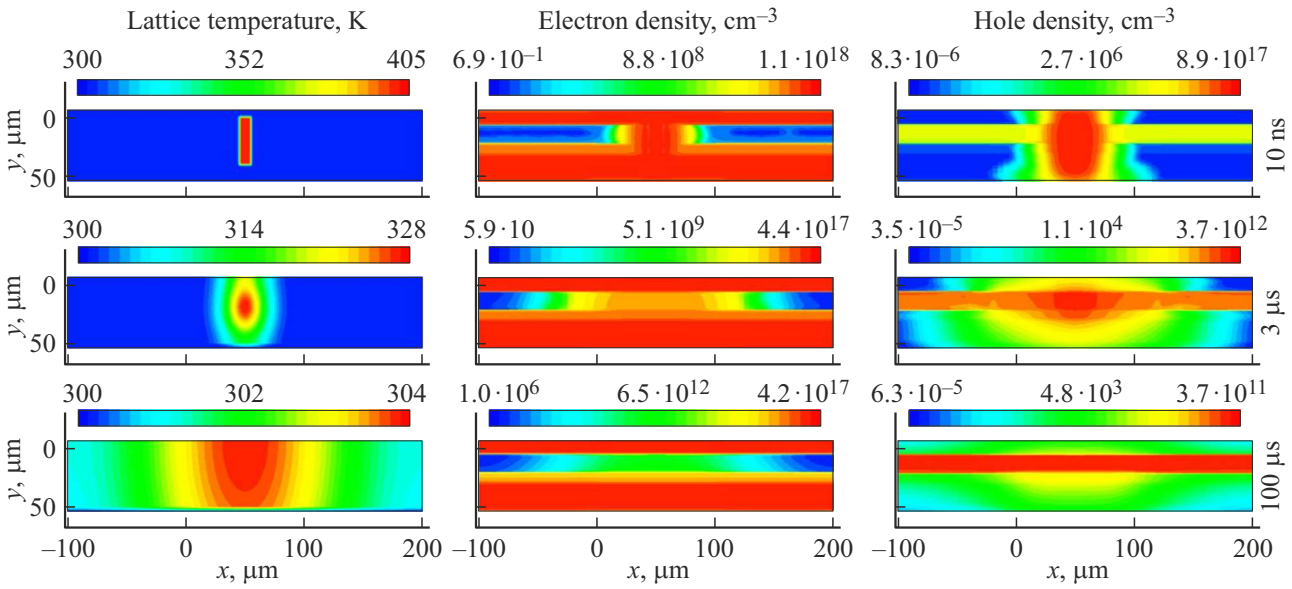

Figure 3. The calculated 2D-distributions of the lattice temperature, concentration of electrons and holes in *S*-diode for the three various time periods from the start of formation of local heated area with the electron-hole plasma. (A color version of the figure is provided in the online version of the paper).

The solution was suggested within the framework of Maxwell-Boltzmann statistics. The approach is justified for studying the long-term dynamics of the redistribution of charge carriers (when their concentration decreases due to recombination by 1–2 orders). It should be emphasized that the heating was provided by the last summand in equation (1). At maximum optical illumination, the rate of heat generation during light absorption was $(\hbar\omega - E_g)G^{\text{opt}} = 4.2 \cdot 10^{10}\,\text{W/cm}^3$.

It should be clarified, that the developed model doesn't describe the process of filamentation in the avalanche *S*-diode. The purpose of the model is to define the way the charge carriers and heat are re-distributed after rapid local generation in a *S*-diode structure. At that, although the optical generation method is artificially introduced, it turns out to be effective when using the TCAD Sentaurus software. Let us proceed to the discussion of the results of numerical modeling.

The temperature and electrons and holes concentration distribution at different time points are shown in Figure 3. It is seen that for 10 kHz frequency, when time between the two switchings is 100 μs, electrons concentration in the channel is higher than concentration of holes by ~ 20 times. For the time of 3 μs (frequency 333 kHz) the ratio between these concentrations in the channel is increased up to 3 orders of magnitude. The calculations demonstrated that the equilibrium concentration of holes in π-domain, exceeding the non-equilibrium concentration is set beyond $\sim 10^{-3}$ s. It shall be clarified that in this study the calculations were made for various values of the electrons capture sections (σ_n). However, the analysis is provided for $\sigma_n = 10^{-19}\,\text{cm}^2$. An increase in the electron capture section leads to a multiple decrease in the time to restore the equilibrium state.

Let's show further that at a certain distance from the initial position of the locally heated area with the coordinate $x = 50\,\mu$m (hereinafter — current filament), an area should be formed where the probability of an avalanche breakdown will be maximum within the sample. The higher the probability, the higher the rate of avalanche generation, which is determined by the expression

$$G_e = \alpha_e n v, \tag{3}$$

where α_e — impact ionization coefficient, n — concentration of non-equilibrium electrons, v — electron velocity.

The impact ionization coefficient is defined by the temperature and electric field. In the study the following dependence is used for the analysis [15]:

$$\alpha_e(E, T) = \gamma a_0 \exp(-\gamma b_0/E),$$
$$\gamma = \tanh\left[\frac{\hbar\omega_{\text{op}}}{2kT_0}\right] \Big/ \tanh\left[\frac{\hbar\omega_{\text{op}}}{2kT}\right], \tag{4}$$

where E — electric field, the values of parameters used: $a_0 = 4 \cdot 10^6\,\text{cm}^{-1}$, $b_0 = 2.3 \cdot 10^6\,\text{V/cm}$, $\hbar\omega_{\text{op}} = 0.035\,\text{eV}$, $T_0 = 300\,\text{K}$.

For the simplicity of the analysis we'll assume that the voltage applied during the second switching doesn't lead to the inhomogeneity of E with respect to x and the dependence $\alpha(x)$ will be defined only by the temperature profile at a given y. We'll calculate α for the intensity of $E = 200\,\text{kV/cm}$, suggesting conventionally that at a given value the switching of *S*-diode begins. Similarly, to simplify the analysis, we'll suggest that $n(x)$ profile is not distorted

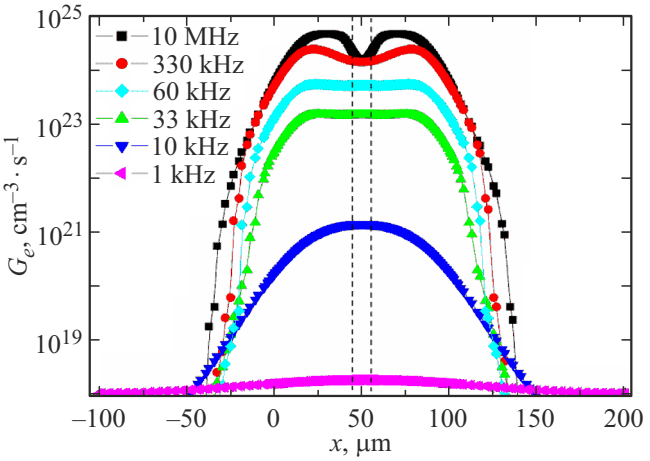

Figure 4. Calculated distributions of efficient rate of the avalanche generation during second switching of *S*-diode for various repetition rates of the two pulses. The dashed lines delineate the current filament area for the first switching of *S*-diode. Coordinate $y = 14\,\mu$m.

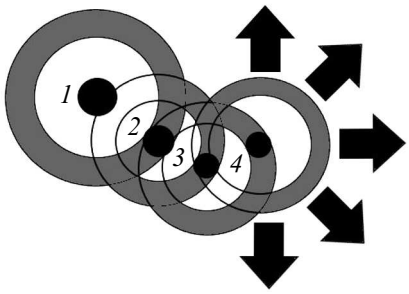

Figure 5. Schematic representation of sequential switching of the four (*1*–*4*) current filaments in the avalanche *S*-diode (top view, see Figure 1, *a*). Black circles — positions of current filaments; grey circles — places corresponding to the maximal rate of G_e after vanishing of the current filament; arrows show possible directions of formation of the next (fifth) current filament within grey circle.

when applying voltage to *S*-diode during the second triggering, while the electron velocity remains constant along x (conventionally, let's select the section of $y = 14\,\mu$m).

Figure 4 illustrates the calculated profile $G_e(x)$ in different moments of time which looks symmetrical. It follows from the figure that an increase in frequency (a reduction in the delay time between two switchings) leads to several characteristic effects. On the one hand, the maximum rate of G_e goes up, which should lead to a decrease of the avalanche breakdown voltage (and switching) of the *S*-diode with the frequency growth. On the other hand, an increase in frequency leads to a change in the coordinate x for the maximum value of G_e (the maximum position can be located in $\sim 15-30\,\mu$m from the initial position of the current filament). And finally, in the middle frequencies band (dozens of kilohertz) we may see in $G_e(x)$ distribution a wide „plateau" up to $60-70\,\mu$m long. The first two effects are qualitatively consistent with the presented experimental data. The presence of a wide area with a constant value of G_e may formally be interpreted as the emergence of a wide channel for current filamentation or the emergence of favorable conditions for synchronous activation of several channels in the „plateau" area. Both options should result in decline of residual resistance of *S*-diode. It should only be emphasized that in our experiments, the maximum switching efficiency is indeed often observed in the range of units-tens of kilohertz (analysis of this effect is not included in the purpose of this paper).

From the presented results, it follows that in the avalanche *S*-diode with the sequential formation of current filaments at high rate the previous diode switching is memorized. In other words, the recharging of deep centers in the vicinity of each previous current filament sets the conditions for the formation of each subsequent switching channel. The mechanism of such switching is schematically shown in Figure 5.

It should be noted separately, that an accurate calculation of the carriers redistribution dynamics during capture to deep centers requires knowledge of many unknown variables: the temperature and field dependences of the electron and hole capture sections, as well as the distribution of the electric field before switching. However, as mentioned above, the sequential switching is not rigidly deterministic, which may be explained by fluctuation of composition. The analysis presented in this paper is aimed at a qualitative explanation of experimental data and outlining a new mechanism for sequential avalanche switching of the current filaments in a structure with deep centers.

5. Conclusion

The studies demonstrated that in the avalanche *S*-diodes — structures with deep centers — filamentation of current leads to formation of a local domain where conditions for the next avalanche breakdown become more beneficial. Such conditions persist for quite a long time, which is associated with the transition to equilibrium filling of deep centers with the charge carriers. At the same time, switching initiated by an avalanche breakdown may not occur for the second time in the current filament area if the lattice temperature is high. Thus, every new filament is formed on the periphery of the previous one, which leads to consequential filling of the entire area of *S*-diodes with the current filaments.

The described mechanism predicts several characteristic features of the frequency dependencies of *S*-diodes parameters, which are planned to be investigated in the future. At this stage, it is important to notice that the identification of this mechanism is of great systematical value for modeling the switching of *S*-diodes. In this regard, we should stress the following:

1) The mechanism makes it possible to justify one-dimensional modeling of double switching of the avalanche

S-diode in the mode of collapsing domains when studying the frequency dependencies of its parameters. At that, in order to match the experimental and calculated results, it is possible, for example, to use the effective fitting parameter — the cross-section of the electron capture to deep centers;

2) the mechanism requires using a new approach to the analysis of experimental dependencies for switching of *S*-diodes at high frequencies (over 1 kHz), since the simulated channel of *S*-diode, in fact, has another (non-equilibrium) structure. It follows from the presented results that before the start of the second switch-on, the concentration of charged iron centers is lower than before the first one. The concentration of free electrons being a way above the holes concentration. As a result, at high frequencies, the channel's conductivity becomes unipolar, since the deep centers do not have time to capture all free electrons after the first switching. In fact, it means that at high frequencies in *S*-diode channel there are no electron-hole junctions (all energy barriers were formed by isotopic junctions between *n*-type layers with various electrons concentration).

Funding

This study was financially supported by the grant of Russian Science Foundation No. 23-29-00053, https://rscf.ru/project/23-29-00053/.

Conflict of interest

The authors declare that they have no conflict of interest.

References

[1] I.A. Prudaev, V.L. Oleinik, T.E. Smirnova, V.V. Kopyev, M.G. Verkholetov, E.V. Balzovsky, O.P. Tolbanov. IEEE Trans. Electron Dev., **65** (8), 3339 (2018). DOI: 10.1109/TED.2018.2845543
[2] I.A. Prudaev, S.N. Vainshtein, M.G. Verkholetov, V.L. Oleinik, V.V. Kopyev. IEEE Trans. Electron Dev., **68** (1), 57 (2021). DOI: 10.1109/TED.2020.3039213
[3] I.A. Prudaev, S.N. Vainshtein, V.V. Kopyev, V.L. Oleynik, S.N. Marochkin. IEEE Electron Dev. Lett., **43** (1), 100 (2022). DOI: 10.1109/LED.2021.3130596
[4] S. Vainshtein, I. Prudaev, G. Duan, T. Rahkonen. Solid State Commun., **365**, 115111 (2023). DOI: 10.1016/j.ssc.2023.115111
[5] S.N. Vainshtein, V.S. Yuferev, J.T. Kostamovaara. IEEE Trans. Electron Dev., **52** (12), 2760 (2005). DOI: 10.1109/TED.2005.859660
[6] S. Vainshtein, J. Kostamovaara, V. Yuferev, W. Knap, A. Fatimy, N. Diakonova. Phys. Rev. Lett., **99** (17), 176601 (2007). DOI: 10.1103/PhysRevLett.99.176601
[7] S.N. Vainshtein, V.S. Yuferev, J.T. Kostamovaara, M.M. Kulagina, H.T. Moilanen. IEEE Trans. Electron Dev., **57** (4), 733 (2010). DOI: 10.1109/TED.2010.2041281
[8] G.M. Loubriel, F.J. Zutavern, H.P. Hjalmarson, R.R. Gallegos, W.D. Helgeson, M.W. O'Malley. Appl. Phys. Lett., **64** (24), 3323 (1994). DOI: 10.1063/1.111266
[9] L. Hu, J. Su, Z. Ding, Q. Hao, X. Yuan. J. Appl. Phys., **115** (9), 094503 (2014). DOI: 10.1063/1.4866715
[10] Y. Sun, L. Hu, Y. Li, L. Zhu, X. Dang, Q. Hao, X. Li. J. Phys. D: Appl. Phys., **55**, 215103 (2022). DOI: 10.1088/1361-6463/ac54d4
[11] V.I. Brylevskiy, I.A. Smirnova, A.V. Rozhkov, P.N. Brunkov, P.B. Rodin, I.V. Grekhov. IEEE Trans. Plasma Sci., **44** (10), 1941 (2016). DOI: 10.1109/TPS.2016.2561404
[12] V. Brylevskiy, N. Podolska, I. Smirnova, P. Rodin, I. Grekhov. Phys. Status Solidi B, **256** (6), 1800520 (2019). DOI: 10.1002/pssb.201800520
[13] M. Ivanov, A. Rozhkov, P. Rodin. Solid State Commun., **379**, 115420 (2024). DOI: 10.1016/j.ssc.2023.115420
[14] I. Prudaev, V. Kopyev, V. Oleinik. Phys. Status Solidi B, **260**, 2200446 (2023). DOI: 10.1002/pssb.202200446
[15] Version H-2013.03 (Synopsis Inc. Sentaurus Device User Guide, Mountain View, CA, 2013).

Translated by T.Zorina